DOI: 10.2478/sspjce-2024-0013

Analysis of Crack Propagation in Composite Materials Using Mixed Finite Elements

Ahmed Bougueroua*, Hamoudi Bouzerd

University 20 August 1955, Skikda, Algeria
Department of Civil Engineering, Faculty of Technology.
*e-mail: ah_ba21@yahoo.fr

Abstract

This study investigates the application of fracture mechanics to analyze cracked structures, particularly focusing on cracks along interfaces in multilayer materials. Assuming perfectly plastic elastic behavior, small displacements, and plane structures, the research employs a new mixed finite element, RMQ-7, derived from Reissner's variational principle. The RMQ-7 element, designed to model both the free edge effect along the crack and continuity in the rest of the material, is used in conjunction with the virtual crack extension method to evaluate the energy release rate and the size of the plastic zone around the crack tip.
Numerical modelling is conducted on various configurations, including plates with central and inclined cracks under different loading conditions. The study concludes that the RMQ-7 mixed finite element is an effective and precise tool for analyzing interface cracks in multilayer materials, providing valuable insights into the mechanical behavior of such structures under stress.

Keywords: fracture mechanics, mixed finite element; rmq-7 element, interface cracks, plastic zone energy release rate.

1 Introduction

The study of cracking has been a significant research focus for several decades. Two primary approaches have emerged: fracture mechanics, which involves a local study of cracks and their progression to fracture, and damage theory, which considers cracking on a global level by analyzing a larger volume of material to study the evolution of microcracks or even cracked material.

Between 1960 and 1980, fracture mechanics gained substantial scientific attention, especially with the advent of nonlinear fracture mechanics, which better accounted for the plastic behavior of materials. Notable works from this period include J.R. Rice in 1968 [1] and D. Bui in 1973 [2], who introduced the concept of contour-independent integrals like the J-integral. These integrals helped characterize the toughness of a material when plasticity extends beyond the crack tip. Additionally, this era saw the first studies on fracture mechanics in multilayer materials [3-4-5]. In this work, we adopt the fracture mechanics approach to study structures with interface cracks under the following assumptions:

- Perfectly plastic elastic behavior of materials
- Small displacements
- Plane structures.

Studying structures with cracked interfaces necessitates the use of specialized mixed finite elements. A new class of mixed finite elements, known as interface elements, emerged by refining Reissner elements using various techniques. For instance, the RMQ-7 element [6], combined with the virtual crack extension method, facilitates the calculation of energy release rate in a single analysis. This element was initially used for identical and different isotropic bimaterials [6] and later for laminate multilayers [7]. An isoparametric formulation of the RMQ-7 element was subsequently developed to model inclined or curved interfaces [8]. Under this formulation, in combination with the virtual crack extension method, the element was used for inclined and curved interfaces [9]. Our work will focus on applying this element to perfectly plastic elastic materials to determine the size of the plastic zone around the crack tip.

Numerous experimental and analytical techniques are available in the literature for determining the size of the plastic zone [10-11-12-13-14-15].

2 Plastic zone around crack tip in two-dimensional medium

2.1 Shape of the plastic zone

The stresses in the vicinity of the crack in mode I (see Figure1) [16]:

$$\begin{gathered}
\boldsymbol{\sigma_{11}} = \frac{\mathbf{K_I}}{\sqrt{2\pi r}}\cos\frac{\theta}{2}\left[1-\sin\frac{\theta}{2}\sin\frac{3\theta}{2}\right] \\
\boldsymbol{\sigma_{22}} = \frac{\mathbf{K_I}}{\sqrt{2\pi r}}\cos\frac{\theta}{2}\left[1+\sin\frac{\theta}{2}\sin\frac{3\theta}{2}\right] \\
\boldsymbol{\sigma_{12}} = \frac{\mathbf{K_I}}{\sqrt{2\pi r}}\sin\frac{\theta}{2}\cos\frac{\theta}{2}\cos\frac{3\theta}{2}
\end{gathered} \tag{1}$$

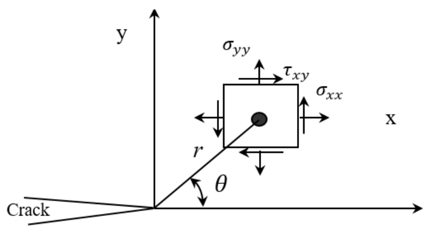

Figure 1: Crack mode I in an infinite plate, definition coordinate system at crack tip

- **Plane stresses**

In plane stresses, the Von-Mises criterion is written [16]:

$$\sigma_y^2 = \frac{1}{2}\left[(\sigma_{11}-\sigma_{22})^2+\sigma_{22}^2+\sigma_{11}^2\right]+3\sigma_{12}^2 \tag{2}$$

By replacing equation (01) in this equation, we obtain:

$$r = \frac{K_I^2}{2\pi\sigma_y^2} cos^2 \frac{\theta}{2} \left(1 + 3\, sin^2 \frac{\theta}{2}\right) \tag{3}$$

When one considers an elastic linear initial state, one writes $\sigma_y = \sigma_e$ elastic limit. Figure 2.a shows the shape of the plasticized area.

- **plane strains**

In plane strains, the criterion of Von-Mises is written in this case [16]:

$$\boldsymbol{\sigma_y^2 = 3\left[(\sigma_{11} - \sigma_{22})^2 + (\sigma_{22} - \sigma_{33})^2 + (\sigma_{33} - \sigma_{11})^2\right] + 18\sigma_{12}^2} \tag{4}$$

With: $\sigma_{33} = \nu(\sigma_{11} + \sigma_{22})$

In the same way, we deduce by replacing equation (01) in equation (02), we obtain:

$$r = \frac{K_I^2}{2\pi\sigma_y^2} cos^2 \frac{\theta}{2} \left((1 - 2\nu)^2 + 3\, sin^2 \frac{\theta}{2}\right) \tag{5}$$

When one considers an elastic linear initial state, one writes $\sigma_y = \sigma_e$.

Figure 2.b shows the shape of the plasticized area.

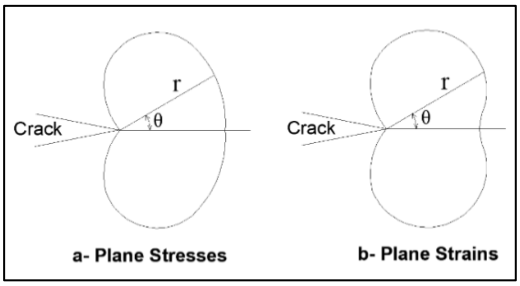

Figure 2: Shape of the plastic zone

2.2 Irwin's approach

This approach fixes an objective[17]: the determination of the stress intensity factor in mode I taking into account the presence of a supposedly small plastic zone in comparison with the length of the crack. (However, strictly speaking of a stress intensity factor in elastoplasticity, does not seem rational); the value thus obtained of this factor K_I will be used to establish an "intrinsic" value ! K_{IC} critical corresponding to elastoplastic fracture.

Irwin therefore supposes an increase in the crack of $r_y \ll a$, and considers that the stress σ_{22} obtained in this zone does not exceed the elastic limit σ_e (perfect elastoplastic constitutive law therefore without hardening). It is therefore a question of estimating the value r_y for a given value of the stress applied to the distance $\sigma_{22\infty}$. From the stress field determined in linear elasticity (equation 02), one writes in mode I and for $\theta = 0$ [16].

$$\sigma_{22}|_{\theta=0} = \sqrt{\frac{K_I}{2\pi r}} \qquad \text{avec} \qquad K_I = \sigma_{22\infty}\sqrt{\pi a} \tag{6}$$

Let us calculate the sum S_1 of the stresses $\sigma_{22}|_{\theta=0}$ between $r = 0$ and $r = r_y$, we obtain:

$$S_1 = \int_0^{r_y} \frac{K_I}{\sqrt{2\pi r}} dr = \sqrt{\frac{2}{\pi}} K_I \sqrt{r_y} \tag{7}$$

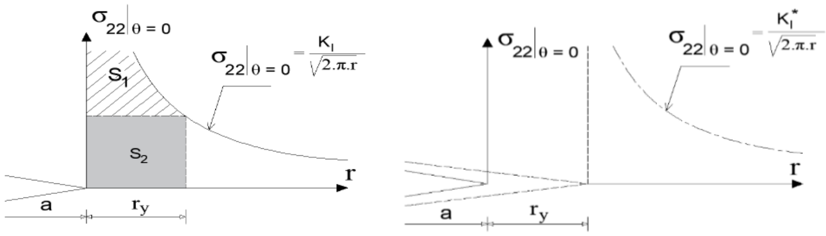

Figure 3: Depth of plastic area

Assuming $\sigma_{22}|_{\substack{\theta=0 \\ r=r_y}} = \sigma_e$, we obtain from equation (06)

$$\sigma_e = \frac{K_I}{\sqrt{2\pi r_y}} r_y = \frac{K_I^2}{2\pi\sigma_e} \tag{8}$$

By replacing equation (08) in equation (07), we write: $S_1 = 2\sigma_e r_y$

If we consider Irwin's hypothesis of perfect plasticity inside the plastic zone, the sum of the stresses corresponds to $S_2 = \sigma_e r_y$

The comparison between (S_1) and (S_2)shows that we must double the depth of the plastic zone to have the same sum of stresses, hence we write:

$$R_y = 2r_y = \frac{K_I^2}{2\pi\sigma_e^2} \tag{9}$$

From the value r_y , Irwin defines a plastic stress intensity factor K_I^* which is written:

$$K_I^* = \sigma_{22\infty}\sqrt{\pi(a + r_y)} \tag{10}$$

3 Numerical modeling

3.1 Presentation of the RMQ-7 element

3.1.1 Use of Reissner's principle

Along a crack one distinguishes two parts, one coherent where it is necessary to ensure the mechanical and geometrical continuity and the other cracked, geometrically discontinuous and incompetent to transmit the mechanical forces due to the loads. To attempt to numerically model this problem by the finite element technique, it is necessary to develop a special element that meets the two requirements above, namely the free edge effect along the cracked part and perfect consistency on the rest. Moreover, it is necessary to take account of the singularity of the stresses at the crack tip.

Classical finite element based on the method of displacement or the method of forces are unable to meet these requirements. This insufficiency led to the use of s two-field methods, because the latter make it possible to act simultaneously on the displacement and stress fields, and can thus solve the problems of continuity and of free edge. In this work, we used the mixed formulation [18] of where all the kinematic quantities (u_i) and all the static quantities (σ_{ij}) appear as explicit variables independently.

3.1.2 Element proposal

Based on Reissner's variational principle, the proposed RMQ-7 element (Figure 4) is rectangular with seven nodes. Three of its sides are compatible with classical linear elements, featuring a displacement node at each end. The fourth side, besides its two kinematic nodes of end, offers three additional nodes: a median displacement node (which will represent the crack tip later) and two intermediate nodes in the middle of each half- side, introducing the components of stress vector along the interface. The continuities of displacement vectors s and stress can be taken into account at this particular side, which must be placed along the interface. In the case of cracked structures, the median node is associated with the crack tip and the static nodes on both sides allowing to satisfy the two essential requirements of such a situation, which are the condition of the free edge on the lips of the crack and the conditions of continuity along the coherent part.

For the configuration final element [6], has developed a new rectangular mixed finite element based on the functional Reissner. It has five nodes and 22 degrees of freedom (Figure 4). Four of these nodes are placed at the ends and each have static and kinematic variables, the fifth node is located in the middle of a horizontal side and has only two cinematic unknown. This element called RMQ-5 will be useful later as a starting point for the construction of the final element. In a first phase, the technique of relocation of degrees of freedom is used to drive of the RMQ-11 member (Figure 4), then in a second phase by static condensation interior degrees of freedom are eliminated to obtain the RMQ-7 element, which will be used to model coherent or cracked interfaces.

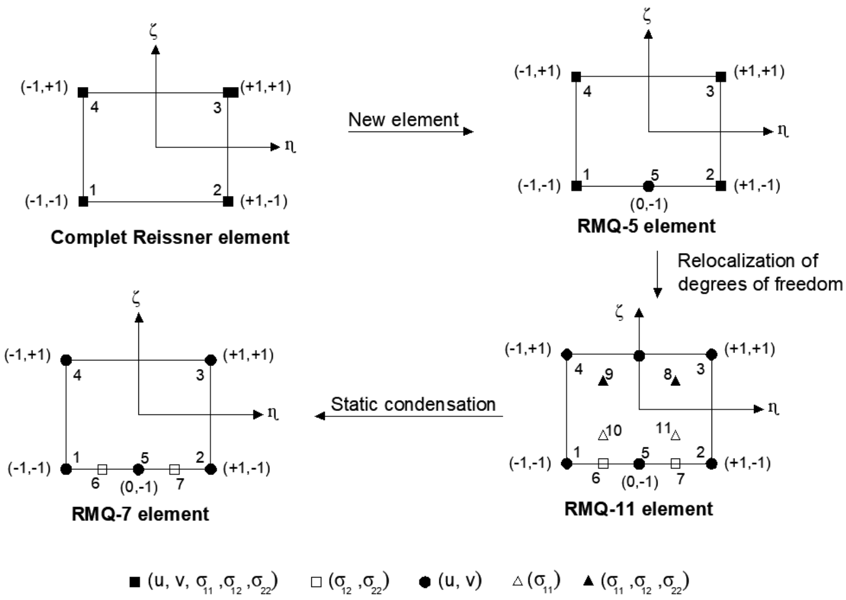

Figure 4: Phases of construction of RMQ-7 element

3.2 Evaluation of the energy release rate G

In this section, we discuss the adaptation of the technique of virtual crack extension to the case of composites laminates with slant crack. The mixed finite element RMQ-7 associated with this technique has shown a good performance in the case of cracked isotropic materials [6] and orthotropic bimaterial [7].
To test its effectiveness in the case of composites laminates with slant crack, we reformulated the implementation of this method to take into account the specificity of this type of structures. In this new formulation, we do not need "the equivalent element" placed in the mesh to represent the initial configuration of the crack. The following steps show how to operate to calculate the energy release rate.

Whereas a change δa of the crack length, leading to a release of an amount of energy $\Delta\Pi$ (where Π represents the deformation energy), the energy release rate G is defined as follows:

$$G = \frac{\delta \Pi(a+\delta a) - \delta \Pi(a)}{\delta a} = \frac{\delta \Pi}{\delta a} \tag{11}$$

The virtual crack extension method [19]is used in this work to evaluate G. Two elements RMQ-7, named crack tip elements (upper and lower), are placed along the cracked interface with the displacement median common node associated with the crack tip (Figure 5a).

The crack length "a" can be increased by an amount Δa acting within strict both elements surrounding the crack tip by a translation of the common node associated with the crack tip without disturbing the surrounding mesh of structure (Figure 5b).

If we consider a small perturbation Δa compared to the dimensions of one of the two elements of crack with the hypotheses (linear elastic behaviour in small displacements) we can write with a good approximation:

$$\mathrm{v}(a) \cong \mathrm{v}(a + \Delta a)$$

Where $\mathrm{v}(a)$ and $\mathrm{v}(a + \Delta a)$are solution vectors of the finite element analysis in the configurations "a" and " $a + \Delta a$ " of the studied structure.

Therefore, the energy release rate G is evaluated from the variations of the stiffness-flexibility matrices in the elements of crack from one finite element discretization using the following equation:

$$G = \sum_{f=1}^{2} \{v\}_f^t \frac{[\Delta K]_f}{\Delta a} \{v\}_f = \frac{\Delta \Pi}{\Delta a} \tag{12}$$

$$With \quad [\Delta \mathrm{K}]_\mathrm{f} = [\mathrm{K}(\mathrm{a} + \Delta \mathrm{a})]_\mathrm{f} - [\mathrm{K}(\mathrm{a})]_\mathrm{f} \qquad (\mathrm{f} = 1,2)$$

Where $[\Delta \mathrm{K}]_\mathrm{f}$ $(\mathrm{f} = 1,2)$ is the variation of the elementary matrix of the element of crack during the variation Δa of the length of the crack, and the subscript f indicates that quantities used are those of crack tip elements only. The other elements are unchanged ($[\Delta \mathrm{K}] = [0]$).

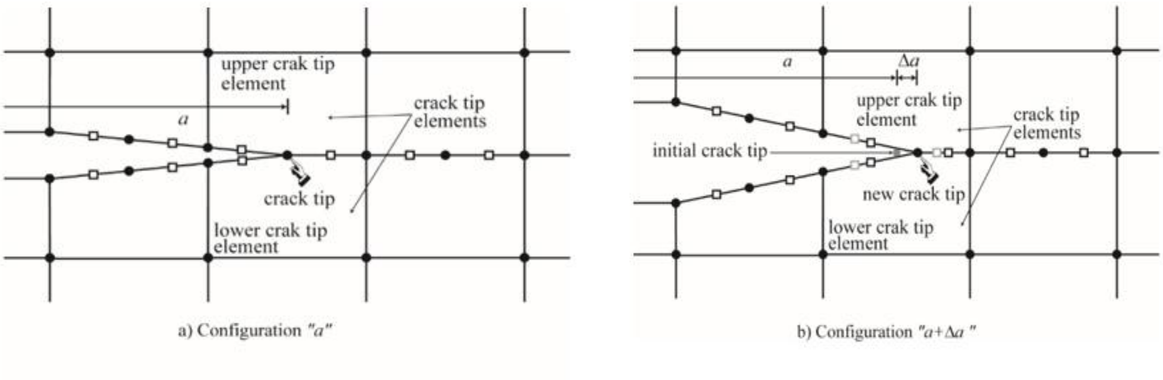

Figure 5: Position of crack tip and length of the crack before and after virtual extension

In practice, the discretization of the cracked structure is performed in the configuration " $a + \Delta a$ " (Figure 4b) of the crack and during the operation of assembly the elementary matrices of the upper and lower crack elements are calculated in the configuration " a" and " $a + \Delta a$ ". The matrices of the configuration " $a + \Delta a$ " are used in the assembly to build the finite element solution $\mathrm{v}(a + \Delta a)$, while the matrices of the configuration " a" do not participate in the assembly and they are stored separately. After the resolution, they will be restored to calculate the energy release rate G by the formula (8).

4 Validation of the proposed model

4.1 Angle cracked plate under tension

The specimen is a plate with inclined center crack, load in tension by $\sigma = 1\ unit$ with the following geometrical: $W = 10\ units$, $a/W = 0.05$. The Young's modulus $E = 100\ units$, the poisson's ratio $\nu = 0.33$ [20]

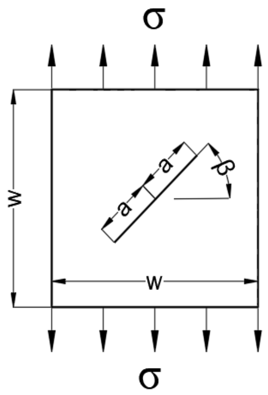

Figure 6: Geometry and loads of an angle-cracked plate under tension.

Table 1 presents the K_I results obtained by RMQ-7 element for different crack inclination angles and compares them with numerical and analytical results.

Table 1: Results for K_I of inclined center crack in a homogeneous, isotropic elastic plate under tension

Crack inclination angle β	RMQ-7	LIU [20]	Error (%)	Exact solution [20]	Error (%)
	K_I	K_I		K_I	
0	1,2746	1.271	-0.28	1.253	-1.72
5	1,2640	1.263	-0.08	1.244	-1.60
10	1,2210	1.238	1.37	1.216	-0.41
15	1,1739	1.194	1.68	1.169	-0.42
20	1,0982	1.126	2.46	1.107	0.79
25	1,0055	1.047	3.96	1.029	2.28
30	0,8995	0.960	6.30	0.940	4.31
35	0,7845	0.853	8.38	0.841	6.72
40	0,6997	0.745	6.08	0.735	4.80
45	0,5787	0.625	7.41	0.627	7.71
50	0,4768	0.520	8.31	0.518	7.95
55	0,4052	0.392	-3.36	0.412	1.66
60	0,3087	0.288	-7.18	0.313	1.37
65	0,2234	0.197	-13.40	0.224	0.28
70	0,1338	0.144	7.08	0.147	8.97
75	0,0803	0.084	4.40	0.084	4.45
80	0,0359	0.036	0.28	0.038	5.65
85	0,0089	0.009	1.11	0.010	11.24

It can be seen that the K_I values calculated using the mixed finite element method are very close to the numerical results (Liu) ant the exact solution, with a difference not exceeding 12% in any case.

4.2 Evaluation of the plastic zone in mode I

The specimen is a plate with central crack, plate of width $B = 100\ mm$, length $L = 200\ mm$ and thickness 2.5 mm.the specimen is an aluminium alloy sheet (2024-T351) with the Young's modulus $E = 73$ GPa , the Poisson's ratio $\nu = 0.3$ and the yield stress $\sigma_Y = 370\ MPa$ [21].

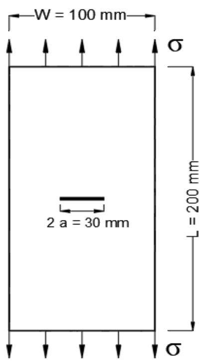

Figure 7: Geometry and loads of plate under tension.

Table 2 gives all the results obtained by different model with the measured plastic zone computed for angle $\theta = 0°$.

Table 2: Size of plastic zone ahead of crack tip ($\theta = 0°$)

Models	RMQ-7	Irwin	Dugdale	Kujawski power law	T.E. Tay [21]	Benrahou [13]
Plastic zone r_y [mm]	0.98	0.88	1.06	0.80	0.84	0.54
Error (%)	0.00	-11.36	7.54	22.5	-16.66	9.25

The calculation of the plastic zone size around the crack tip using the RMQ-7 element (a mixed finite element) according to the Von Mises plasticity criterion shows good concordance with values calculated by Irwin's model, with an error not exceeding 12%. The error ranges from 7% to 16% for the models of Dugdale, Benrahou, and Tay. However, the error is around 22% when compared to the Kujawski model.

4.3 Evaluation of the plastic zone bi-axial case of loading

In the numerical calculation , a plate width of 2W and 2L length having a central crack 2a [22] is used to investigate the size of the plastic zone in the vicinity of the crack tip under a load voltage bi- axial σ, as shown in figure 8 . The plane stress condition is assumed. The plate being symmetrical, only a quarter of the plate is modeled.

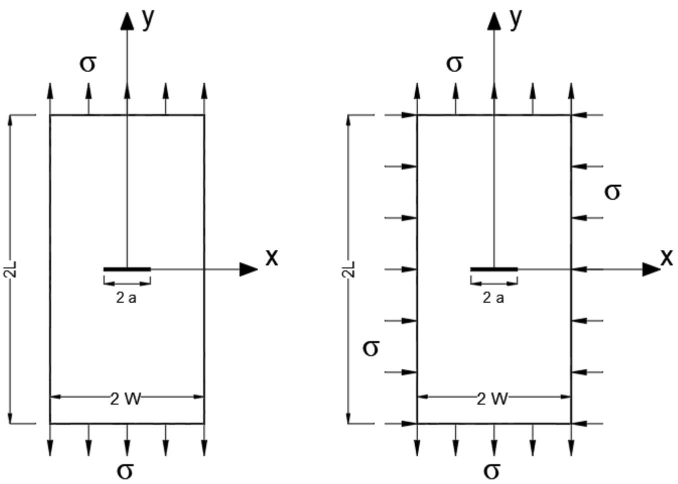

Figure 8: A center cracked plate in tension a) the case to uniaxial stress (transverse stress is zero); b) the case to uniaxial stress (transverse is compressive stress, which is equal to tensile stress).

The material is supposed to have a perfectly plastic elastic stress-strain relationship, the Von-Mises criteria are used in the calculations. The Young's modulus E is 210 GPa and the Poisson's ratio v is 0.3 [22].

4.3.1 Case of the uniaxial stress (the transverse stress is zero)

Table 3: The results of R_y calculated by the three methods in the case of $\lambda = \sigma_{xx}/\sigma_{yy} = 0$.

σ [Mpa]	σ_s $[Mpa]$	a/W	a $[mm]$	R_y by RMQ7 $[mm]$	R_y by MCOD $[mm]$[22]	Error (%)	R_y by Irwin $[mm]$ [22]	Error (%)
60	235	0.067	10	0.2945	0.3082	4.44	0.2995	1.66
60	255	0.067	10	0.2430	0.2599	6.50	0.2531	3.99
60	275	0.067	10	0.2230	0.2225	-0.22	0.2167	-2.90
60	300	0.067	10	0.1730	0.1863	7.13	0.1814	4.63
60	235	0.125	17	0.5125	0.5277	2.88	0.5092	-0.64
40	325	0.1	10	0.0650	0.0694	6.34	0.0678	4.12
40	350	0.1	10	0.0550	0.0594	7.40	0.0584	5.82
80	375	0.1	10	0.1950	0.2129	8.40	0.2070	5.79
80	400	0.1	10	0.1850	0.1866	0.85	0.1814	-1.98
80	350	0.143	17	0.3850	0.4215	8.65	0.4054	5.03

The results obtained from the size of the plastic zone Ry by the element RMQ-7 are compared with the results by the MCOD method and by the Irwin formula, it can be seen that the results of Ry calculated by the mixed finite element RMQ -7 are very close to those of Irwin and the method of MCOD where the difference does not exceed in any case 6%.

4.3.2 Case of uniaxial stress (transverse is the compressive stress, which is equal to the tensile stress)

Table 4 show the results of R_y calculated by the three methods in the case of $\lambda = \sigma_{xx}/\sigma_{yy} = -1$

Table 4: The results of R_y calculated by the three methods in the case of $\lambda = \sigma_{xx}/\sigma_{yy} = -1$

σ [Mpa]	σ_s $[Mpa]$	a/W	a $[mm]$	R_y by RMQ7 $[mm]$	R_y by MCOD $[mm]$[22]	Error (%)	R_y by Irwin $[mm]$[22]	Error (%)
30	305	0.100	12	0.0900	0.1011	10.97	0.0988	8.90
40	355	0.100	12	0.1300	0.1305	0.38	0.1274	-2.04
50	355	0.100	15	0.2300	0.2458	6.42	0.2412	4.64
60	275	0.100	16	0.5500	0.5904	6.84	0.5819	5.48
60	275	0.083	14	0.4900	0.5158	5.00	0.5092	3.77
80	325	0.083	15	0.7100	0.6987	-1.61	0.6864	-3.43
90	400	0.083	20	0.7900	0.7817	-1.06	0.7710	-2.46
100	400	0.083	20	0.8800	0.9607	8.40	0.9429	6.67
80	325	0.125	17	0.7500	0.7973	5.93	0.7779	3.58
60	300	0.111	18	0.5500	0.5643	2.53	0.5559	1.06
70	270	0.091	11	0.5800	0.5686	-2.00	0.5564	-4.24

The results obtained for the size of the plastic zone Ry by the model with the element RMQ-7 are compared with the results by the MCOD method and by the Irwin formula. It can be seen that the results of Ry calculated by the mixed finite element RMQ -7 are close to those of Irwin and the method of MCOD where the difference does not exceed in any case 9 %.

5 Conclusion

This work highlights the efficacy of the RMQ-7 mixed finite element in the analysis of interface cracks in multilayer materials. By utilizing Reissner's principle, the RMQ-7 element successfully models the mechanical and geometrical continuity required for accurate fracture analysis. Validation against experimental and analytical results demonstrates the element's reliability in predicting stress intensity factors and plastic zone sizes. The study confirms that the RMQ-7 element is a robust tool for fracture mechanics applications, offering precise insights into the behavior of cracked structures under various loading conditions.

References

[1] Rice, J. R. (1968). A Path Independent Integral and the Approximate Analysis of Strain Concentration by Notches and Cracks. *Journal of Applied Mechanics*, 379-386.

[2] Bui, H. (1974). Dual path Independent Integral in the boundary value problems of crack. *Engineering Fracture Mechanics*, *6*, 287-296. https://doi.org/10.1016/0013-7944(74)90027-7

[3] Sih, G., & Rice, J. (1964). The Bending of plates of Dissimilar Materials With Cracks. *Journal of Applied Mechanics*, *31*, 477-482. https://doi.org/10.1115/1.3629665

[4] Erdogan, F. (1965). Stress Distribution in Bonded Dissimilar Materials Containing Circular or Ring-Shaped Cavities. *Journal of Applied Mechanics*, *32*(4), 829-836. https://doi.org/10.1115/1.3627323

[5] Comninou, M. (1977). The Interface Crack. *Journal of Applied Mechanics*, *44*(4), 631-636. https://doi.org/10.1115/1.3424148

[6] Bouzerd, H. (1992). *Mixed finite element for cohesive or cracked interface*. Doctoral Thesis. Claude Bernard University, Lyon I, France.

[7] Bougueroua, A. (2006). *Delamination propagation in laminates*. Master’s Thesis. University 20 August 1955, Skikda, Algeria.

[8] Bouziane, S. (2009). *Mixed finite element for cracked interfaces in anisotropic bimaterials*. Doctoral Thesis. University 8 May 1945 , Guelma , Algeria.

[9] Bouziane, S., Bouzerd, H., Boulares, N., & Guenfoud, M. (2014). Energy release rate for kinking crack using mixed finite element. *Structural Engineering and Mechanics*, *50*, 665-677. https://doi.org/10.12989/sem.2014.50.5.665

[10] Huang, X., Liu, Y., & Huang, X. (2019). Analytical characterizations of crack tip plastic zone size for central-cracked unsti ff ened and sti ff ened plates under biaxial loading. *Engineering Fracture Mechanics*, *206*, 1-20. https://doi.org/10.1016/j.engfracmech.2018.11.047

[11] Fernando, L., Marques, N., Antonio, M., Tupiassú, J., Castro, P. De, & Fernando, L. (2020). Elastoplastic 3D analyses of plastic zone size dependencies on load-to-yield strength and on crack size-to-width ratios under mixed mode I / II. *Theoretical and Applied Fracture Mechanics, 107,* 102490. https://doi.org/10.1016/j.tafmec.2020.102490

[12] Kumar, K. G., Silpa, V. J. K., Vamsi, B. V. S. R., & Bhadauria, S. S. (2018). Studies on the Critical Size of the Plastic Zone in Pure Mode-I and Mixed Mode (I / II) Fracture. *Materials Today: Proceedings, 5*(2), 7765-7774. https://doi.org/10.1016/j.matpr.2017.11.454

[13] Benrahou, K. H., Benguediab, M., & Belhouari, M. (2007). Estimation of the plastic zone by finite element method under mixed mode (I and II) loading. *Computational Materials Science*, *38*, 595-601. https://doi.org/10.1016/j.commatsci.2006.04.001

[14] Heung-Bae, P., Kyung-Mo, K., & Byong-Whi, L. (1996). Plastic zone size in fatigue cracking. *International Journal of Pressure Vessels and Piping*, *68*(3), 279-285. https://doi.org/10.1016/0308-0161(95)00066-6

[15] Tieying, W., Danièle, W., & Daniel, K. (2016). Analysis of the plastic zone of a circle crack under very high cycle fatigue. *International Journal of Fatigue*, *93*, 415-421. https://doi.org/10.1016/j.ijfatigue.2016.08.021

[16] Naman, R. (1995). *Rupture par Fissuration des Structures* (Hermès). Paris, France

[17] G.R Irwin. (1963). Structural aspects of brittle fracture. *AGARD 17th S and M Panel Meeting, Applied Materials Research*, 65-81.

[18] Reissner, E. (1950). On variational theorem of elasticity. *Journal of Mathematics and Physics*, 90-95. https://doi.org/10.1002/sapm195029190

[19] D.M. Parks. (1974). A stiffness derivative finite element technique for determination of crack tip stress intensity factors. *International Journal of Fracture, 10*, 478-502. https://doi.org/10.1007/BF00155252

[20] Liu, X. Y., Xiao, Q. Z., & Karihaloo, B. L. (2004). XFEM for direct evaluation of mixed mode SIFs in homogeneous and bi-materials. *international journal for numerical methods in engineering*, *1118*, 1103-1118. https://doi.org/10.1002/nme.906

[21] TAY, T. E., YAP, C. M., & TAY, C. J. (1995). Crack tip and notch tip plastic zone size measurement by the laser speckle technique. *Engineering Fracture Mechanics*, *52*(5), 879-893. https://doi.org/10.1016/0013-7944(95)00060-9.

[22] Yi, H., Jingjie, C., & Gang, L. (2010). A new method of plastic zone size determined based on maximum crack opening displacement. *Engineering Fracture Mechanics*, *77*(14), 2912-2918. https://doi.org/10.1016/j.engfracmech.2010.06.026.